Journal of Engineering and Sustainable Development
https://jeasd.uomustansiriyah.edu.iq/index.php/jeasd
https://doi.org/10.31272/jeasd.27.4.10

Vol. 27, No. 04, July 2023
ISSN 2520-0917

Original Research

STRUCTURAL PERFORMANCE OF COMPOSITE BOX BEAMS WITH CORRODED BOTTOM FLANGE UNDER MONOTONIC AND REPEATED LOADS

Ghufran Khudair Abbass*, Ali Hameed Aziz

Civil Engineering Department, College of Engineering, Mustansiriyah University, Baghdad, Iraq

Received 26/07/2022 ***Accepted in revised form 15/11/2022*** ***Published 01/07/2023***

Abstract: The current research is dedicated to studying the flexural behavior of composite box beams with corroded bottom flanges. Six simply supported beam specimens were manufactured and tested. The composite box beams were fabricated with steel box beams of 1100mm, 100mm, and 100mm for length, width, and height, respectively, while the concrete deck slabs were made with dimensions of 1100mm, 400mm, and 50mm for length, width, and thickness, respectively. The composite sections were formed by connecting the RC deck slabs with the steel box beams by using a headed shear connector. Three main variables were considered; the load type (monotonic or repeated), bottom flange thickness (with or without corrosion), and whether to consider or ignore the strengthening by CFRP strip. Experimental results indicated that the ultimate loads were decreased by 29-33% for the corroded bottom flange beam specimens; while the ultimate loads for the strengthened beam specimens were increased by 60-67% as compared with the un-strengthened corroded corresponding beam specimens. Also, the change of the applied loads from monotonic to repeated leads to a reduction of the ultimate load by 17-22%.

Keywords**:** *Composite sections; box beam; corrosion; Carbon fiber reinforced polymer; monotonic loads; repeated loads*

1. Introduction

In relation to this research, the composite beam is built-up of a reinforced concrete deck slab and steel beam (I-section, box section, hybrid…. etc.) joined together by using mechanical shear connectors (compositely). It has been demonstrated that using a composite beam that resists load as a unit can frequently support 33 to 50 percent or more load than a steel beam alone in non-composite (no mechanical bond of shear from the slab to beam or shear transferring across the common interference) [1]. Shear connectors that give a mechanical bond that transfers the horizontal shear between the two interference materials have a provisional factor to have a composite member. In recent decades, however, composite structural members have been adopted and widely used since the 1950s, especially for highway bridges [1]. Presence the of corrosion in steel bars and steel plates which were used to fabricate the structural and non-structural elements such as buildings, bridges, machines, and any other steel structures leads to harmful and passive effects on the architectural and structural performance [2]. This problem should be taken into account throughout the planning, studying, and designing stages of any project. Each year, about 20% of the production of steel and iron is used to compensate for the metallic materials that have been abandoned because of rust, which leads to corrosion [2].

**Corresponding Author*:
eama005@uomustansiriyah.edu.iq

The increasing concentration of the molarity of sulfuric acid means the rate of corrosion will increase; for example, steel with high phosphor content has a high corrosion rate [2]. Referring to (ACI 440.4R-04), the beams reinforced with CFRP have the same flexural behavior when they are reinforced with steel. The brittle nature of FRP should not be ignored because it doesn't have a yield point. In addition to limited research, however, the strength and lightness make this material suitable for construction manufacture [3].

Ahmed, (2001) [4], prepared research devoted to a new system that combines the utilization of corrugated steel plates as webs for plate or box girders, and its advantages in contrary to the usual flat plate. The flexural strength of the beam is merely provided by the flanges of the new system with no participation from the corrugated web, which provides the shear capacity of the system. The shear behavior of girders with corrugated webs is discussed in this research, in addition to the torsion behavior of composite box girders with corrugated steel webs. Two structural characteristics concluded the investigation:

-The contribution of the corrugated web to the moment capacity and then its effects on the flexural strength of the composite steel-concrete beam is inconsiderable, and it can be completely dependent on the flange yield stress.

-There is no interaction between the flexural behavior and the shear behavior of the composite steel-concrete beam with a corrugated steel web. The shear strength is provided merely by the web, which is controlled by buckling.

Abdullah, et al (2004) [5], studied experimentally the performance of composite steel I-beams with a damaged bottom flange (tension zone) and strengthened them by using CFRP plates. Six beam specimens of composite steel-concrete beams were manufactured and tested. The composite beams were made with I-steel section type (W8x12), grade (A572) with (2.4m) length, and a concrete deck slab of (812mm) width and (76mm) depth connected directly by shear connectors to the top flange of the steel I-section beam. The experimental work includes two intact steel beams (reference steel beams) and four specimens of composite steel beams damaged by cutting part of the bottom flange thickness on the assumption of causing corrosion and then strengthened with CFRP plate. All beam specimens were tested under four-point loads with a clear span of (3.05m). Test results found that the strength and stiffness of the strengthened damaged composite beams were increased significantly.

Qing, et al (2005) [6], established a three-dimensional finite element model to study the flexural and shear behavior of simply supported composite beams subjected to combined bending and shear and then to evaluate the participation of the concrete slab and composite action at the moment and shear endurance of the composite beam. The numerical investigation was done by using ABAQUS finite element software. Numerical results indicate that the vertical shear strength of composite beams increases with an increase in the degree of shear connection.

Amer, and Qussay, (2013) [7] carried out the numerical study using a nonlinear finite element computer program. ANSYS (version-12) to analyze the structural behavior of composite steel-concrete beams and compare the results with obtainable experimental tests. A three-dimensional finite element model was

developed. The factors that were achieved in this study investigation included the effect of the number of shear connectors, concrete grade (compressive strength f'_c) ratio of thickness to the width of the concrete slab, yield strength of steel beam (fy), and the effect of ultimate load for the shear connector. The geometry and details of the cross-section for the composite beam under study were (5490mm) for length, composed of a reinforced concrete slab of (1220mm) width and (152mm) thickness, connected by the shear connector to the top flange of a steel I-section beam of (152mm) width and (18mm) depth. The depth of the steel I-section was (305mm) with a web thickness of (10mm). The external concentrated load was applied at the mid-span of the simply supported composite beam.

AZ. Muhammad, (2014) [8] investigated the effect of soil properties on the corrosion of carbon steel pipelines. In this research about (180) samples of carbon steel plate were embedded in different types of soil conditions for at least five months to achieve the actual corrosion rate. PH value of the soil condition with less than (0.05) is the essential parameter in corrosion rate. For data analysis, the weight loss method was used because it was simple and practical and the results are quite good. There were many factors that affected the rate of corrosion of steel plates embedded in the soils. Generally, such as alkalinity, hardness, and PH value, for example, water with a low PH value is confirming the corrosion, while with a high PH value calcium carbonate is more possible to deposit a shell and reduce the corrosion. Bacteria are another factor causing and expediting corrosion.

Amanda, et al (2018) [9] studied the structural behavior of the corroded steel girders by using a 3D finite element model built in ABAQUS. In addition to experimental testing, the investigation is emphasizing the effects of web area loss of the steel girder and web thinning on the load capacity, and the impacts of location, size, and shape of the area loss upon the shear and web buckling resistance. Four types of specimens were prepared and tested by compression test setup to evaluate the influences of web area loss and web thinning on the behaviors of the girder. The experimental results data contained the stress-strain relationship, the ultimate strength before failure, and deformation measurements. Specimen type (1) was used as a reference, type (2) consisted of corroded steel specimens simulating the web thinning effect, and type (3) contained steel specimens with different sizes, shapes, and locations of the losing area to simulate the web area loss and the fourth type included corroded steel girder specimens with the web area loss for simulating the combined influence of web thinning and area loss. The last type is approaching the actual status of steel girder deterioration.

Amer, et al (2019) [10] studied the flexural behavior of composite concrete slab-box section steel beams. The experimental work was performed to examine and study the effect of using different steel tube (box) section shapes (hexagonal, square, and rectangular) with the same shear connector type (headed stud or angle stud, or perfobond) on the flexural behavior of the composite beams, and also to investigate the flexural behavior of those beams under the influence of using the different types of shear connectors on the same tube section shape. Eighteen composite concrete slabs with tube

(box) steel beams were fabricated and tested through distributing them into two groups. Each group contained nine specimens. The first group focalized on the three types of steel section, each of them with the same shear connector type, while the second group specified the testing of every type of steel section with the three types of shear connectors. The geometric shapes and dimensions of the composite beams with the following main unified dimensions and properties for all of the specimens the same reinforced concrete slab dimension (200x400x130mm), steel tube thickness of (2mm), yield and ultimate stress of (322 MPa) and (390 MPa) respectively, depth of all steel tube section was (100mm). Test results show that:-

1. The steel tube section shapes (hexagonal, square, and rectangular) were adopted for engineering construction utilities practically, improving and supporting and supporting the nature of services for the building, providing a distinguished strength and stiffness starting by (114 kN) for hexagonal shape to research up to (170 kN) for rectangular shape which means that it provides a better structural characteristic because of higher effective area of its steel section.

2. Higher strength and then the ultimate load were provided by using the perfobond shear connector type, (6.25% to 9.74%) compared with the headed stud shear connector and (3.66% to 9%) compared with the angle shear connector, moreover, the demanded load for obtaining the beam slips with perfobond shear connector where higher than the loads required for the beams with a headed stud and angle shear connectors.

2. Research Significant

Sometimes, the composite steel-concrete sections are subjected to local damage due to several reasons, such as overload, earthquake, sulfate attack, etc., which lead to local retardation in their structural function. The current study concerns the structural behavior of the composite steel-concrete box beams with corroded bottom flanges. Therefore, the mechanism of action of corroded bottom flange composite beams and the extent to which they bear the applied forces are almost unknown, not well understood, and not covered in the past literature.

3. Experimental Work

3.1 Experimental program

The experimental work consists of manufacturing and testing six simply supported composite steel-concrete box beam specimens as well as a series of control specimens (cubes, cylinders, and prisms) to assess the mechanical properties related to fresh and hardened concrete. Three main parameters have been adopted; type of loading (monotonic or repeated); bottom flange thickness (with or without corrosion) and strengthening by CFRP strip (considered or ignored).

3.2. Beam Specimens Description

The steel box section was manufactured by using (2mm) steel plate bent by using a bending machine (press machine) to form the required shape, which consists of five steel plate pieces; two vertical steel webs with (1100x100mm) dimensions were connected at the bottom by one bottom steel flange of (1100x100mm) dimensions, and at the top, each web was connected by one steel top flange (wings to the right and left sides) expanded along the width of (50mm). To prevent the local failure of the steel

box section at the ends (supports), three pieces of steel plate with dimensions of (100 x 2mm) have been welded on each support zone at a distance of (50mm) apart, starting from the end of the beam at (90^{o}) within the longitudinal axis of each beam. The six beam specimens comprised of reinforced concrete slabs were poured with normal strength concrete (NSC) by the usual shuttering procedure and bonded compositely with the top flanges of the steel box beams by using a headed stud (screw) shear connector. The beam specimen deck slabs have a typical rectangular shape with a dimension of (1100x400x50mm) for the length, width, and thickness respectively, and are cast with one layer of longitudinal and transverse reinforcement placed at the bottom of the slab with a concrete cover of (10mm). The longitudinal reinforcement consists of (5Ø6mm) steel deformed bars distributed equally in the transverse direction; while (13Ø4) deformed steel bars were used as transverse reinforcement and distributed equally in the longitudinal direction. Table 1 and Fig.1 show the description and details of the tested specimens.

Table 1. Description of Tested Beam Specimens

Beam Coding	Loading Type	Bottom Flange	Strengthening by CFRP
BMF	Monotonic	Un-corroded	None
BMCF	Monotonic	Corroded	None
BMCSF	Monotonic	Corroded	CFRP
BRF	Repeated	Un-corroded	None
BRCF	Repeated	Corroded	None
BRCSF	Repeated	Corroded	CFRP

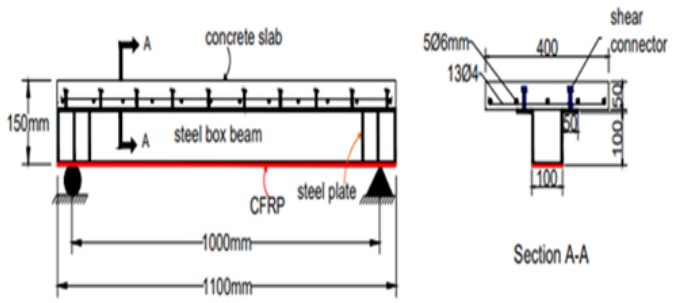

Figure 1. Beam Specimen Details

3.3 Materials

Many materials were used to manufacture and create both, the beam specimen and control samples. Ordinary Portland cement (type I) conformed to Iraqi Specification No.5/1984 [11]; natural sand passing through a sieve size of (4.75mm) conformed to the Iraqi standard Specification No.45/1984 [12]; crushed gravel with a maximum size of (12mm) conformed to Iraqi Specification No.45/1984[12]; High range water reducing admixture (superplasticizer) type (Viscocrete5930) conformed with ASTM C494/C494M-99a [13] were used to produce concrete mixes. (Ø6mm) and (Ø4mm) steel deformed bars conformed to ASTM A370-02 [14], were used as longitudinal and transverse reinforcement, respectively. The tensile strength of the used steel tubular columns was tested by using steel plate strips of thickness (2mm) conformed to ASTM A615/A615M-86a [15]. Carbon fiber reinforced polymer (SikaWrap-300C) tap with (50cm) width was used for the external strengthening of tested beam specimens. Epoxy resin (sikadoure-330) was used to stick the CFRP at the bottom flange of the steel box beam.

3.4 Mix and Cast Concrete

One concrete mix with (530 Kg/m^3) cement, (673 Kg/m^3) sand, (912 Kg/m^3) gravel, (201 Liter/m^3) water and (0.4 Liter/m^3) HRWR was

used throughout the present study. The row materials and admixtures of the adopted concrete mix were mixed using a rotary mixer with a capacity of ($0.2m^3$). Six wooden molds were made by using plywood with inside dimensions of (400x50x1100mm) were used to produce the concrete deck slab which represents a major part of the composite box beam. The wooden molds were fixed to the top of the steel box beams by using steel screws (shear connectors). The inner faces of the molds were oiled to make the stripping process of the specimens easier; then, before pouring the concrete mix, the necessary reinforcements were placed inside the wooden mold. As soon as the concrete mixing process is completed, the pouring process is started by placing the concrete mix in the mold which was prepared to get a deck slab (50mm) thick. After the casting process is completed, the specimens were placed on the table vibrator for compaction purposes, and then left on laboratory conditions. After 2 days, the wooden molds were removed from the concrete specimen and cured by using wet burlap for 28 days.

Figure 2. Beam Specimen Deck Slab Cast

3.5 Fresh and Hardened Concrete Tests

The wet concrete unit weight (Density) test was performed for the fresh concrete using a cylinder with dimensions of (100×200mm) according to (ASTM-C138) [16]. While, the cube concrete compressive strength (f_{cu}) test, cylinder concrete compressive strength (f'_c) test, splitting tensile strength (f_t) test, flexural tensile strength (f_r) test, and dry unit weight ($\gamma_{c\text{-}dry}$) test were carried out after the (28days) of concrete curing according to (BS1881-116-1983) [17], (ASTM C39/C39M-01) [18], (ASTM C496M-04) [19], (ASTM C78-02) [20] and (ASTM C138) [16] respectively. Test results were summarized and provided in Table 4.

Table 2. Test Results of Fresh and Hardened Concrete

Property	Value
f_{cu}(MPa)	46.6
f'_c (MPa)	38.28
f_r (MPa)	3.10
f_t (MPa)	2.64
γ_D (Kg/m^3)	2356
γ_w (Kg/m^3)	2388

3.7 Corrosion Process

As mentioned in the experimental program, four box beam specimens were made with corroded bottom flange; therefore, four beam specimens were subjected to rapid corrosion by being laid in a polyethylene circular basin of (1.5m) diameter, containing a diluted sulfuric acid solution with (10%) concentration, Fig. 3.

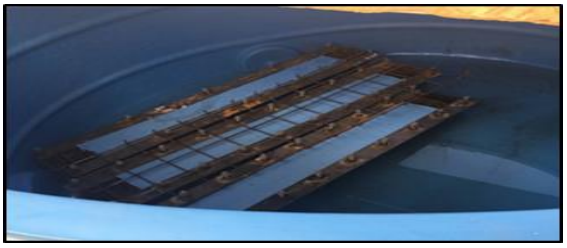

Figure 3. Beam Specimens in basin contained a diluted sulfuric acid solution

To create the local corrosion for the bottom flanges alone, the height of diluted sulfuric acid solution at the basin was not more than (1cm) for a time of subsequently the specimens were

brought out the basin and exposed to the normal environment (humid air and oxygen) to have a corroded condition of the bottom flanges, the condition which was actually occurred. As second stage, the specimens were embedded on a natural agricultural moist soil which has a low clay content for about (38 days), by excavating a shallow groove of not more than (2cm) depth for each specimen (to ensure exposing the bottom flange of the steel box beam only), and adding a diluted sulfuric acid solution of (10%) concentration to increase the acidity environment of the soil moisture content and reduce the (PH) value, Fig.4.

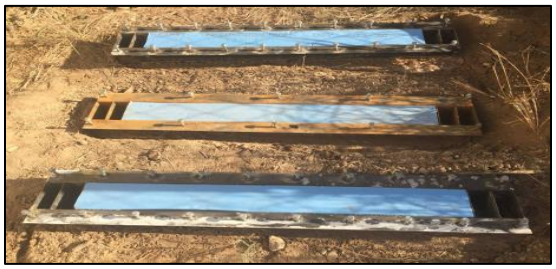

Figure 4. Beam Specimens in soil with a diluted sulfuric acid solution

The impact of corrosion, due to exposure to an acidic medium and normal environment, leads to reduce the bottom flange thickness by (41%).

3.8 Strengthening Process

As mentioned in the experimental program, two of the four corroded bottom flange specimens, (BMCSF) and (BRCSF), were strengthened by using CFRP strips. As a first step, the corroded layers were removed from the substrate by using an electric steel brush and cleaned of any debris, dust, foreign particles, etc. Then, the strain gauges were fixed on the bottom flange of each specimen for the subsequent testing requirements and were protected by a silicon pad before applying the epoxy resin. Then, the CFRP pieces were prepared to the required dimensions of (1100x100mm) by cutting the CFRP fabric by a scissor, Fig. 5.

Figure 5. Strengthening of corroded bottom flange by CFRP Strip

The final step is preparing the epoxy resin by mixing two components thoroughly for about five minutes, and then the prepared epoxy resin is used directly onto the substrates as the first layer by an ordinary brush. Then the CFRP pieces are attached carefully to the applied epoxy resin and smoothened by hand and derive out any irregularities or air pockets by using a hand steel roller until the resin was squeezed out of the slots of the fabric. Finally, another thin layer of epoxy resin was applied on the CFRP strip, and the specimens were left out for not less than 2 weeks for curing and hardening of CFRP.

3.9 Instrumentation and Measurements

All specimens were tested using a hydraulic universal testing machine (MFL system) with an ultimate load capacity of (3000kN). To measure the vertical deflection, dial gauges with an accuracy of (0.01mm/div.) were used. For each tested beam specimen, the dial gauges were fixed at the bottom flange face, one at the mid-span and the other at a quarter of the span. Strain gauges were used to evaluate the performance of the concrete deck slab and steel box beam and to measure the deformations of reinforced concrete and steel box beam during the load application. An automatic data logger

instrument of type (TML/ TC-32K) was used to convert the electrical signal emanating from strain gauges to a corresponding strain reading. The strain gauges were fixed in four different locations, as shown in Table 3.

Table 3. Distribution of the strain gauges

Gauge No.	Location	
1&2	Bottom Flange	Mid-span (L/2) Quarter-span (L/4)
3	At mid span, mid-height on the web side of steel box beam	
4	Top face, at the center of the RC deck slab	

Figure 6. Data logger and location of strain gauges

3.10 Test Setup

Six simply supported beam specimens of composite concrete- steel box section with (1000mm) clear span, were tested by a universal testing machine under one monotonic or repeated concentrated load. For the monotonically tested beam specimens (BMF), (BMCF), and (BMCSF) the tests were done directly. While for repeatedly tested beam specimens (BRF), (BRCF) and (BRCSF), the maximum repeated load was taken as (78%) of the ultimate load capacity of monotonically tested reference beam specimens (BMF), and applied in three cycles increments until failure. As a first step, the tested beam specimens were arranged and adjusted so that the supports, applied load, and instruments were in their correct location. Then, the load is applied gradually with a constant rate of (5 kN) up to the failure state. At the end of each load increment, all test observations and measurements for the vertical deflection, strains, and deformation development on the surface of the tested beam were recorded. When the tested beams reached an advanced stage of loading, smaller increments were applied until failure. All tests photos and measurements were recorded, marked, arranged, and analyzed to be presented and discussed in the next articles.

4. Test Results and Discussion

4.1 Ultimate load capacity (P_u)

The ultimate load capacity of the tested beam specimens was summarized and provided in Table 6. For the beam specimens which were tested under the effect of monotonic load, the ultimate loads were (90kN), (60kN), and (100kN) for the beam specimens (BMF), (BMCF), and (BMCSF) respectively. While, for the beam specimens which were tested under the effect of repeated loads, the ultimate loads were (70kN), (50kN), and (80kN) for the beam specimens (BRF), (BRCF), and (BRCSF) respectively. From the above results, it can be seen that the obtained results are proportioned to the state of each tested beam specimen.

4.2 Effect of Corrosion on (P_u)

As mentioned before, the impact of corrosion, due to exposure to an acidic medium and normal

environment, leads to reduce the bottom flange thickness by an average (of 41%). The flexural behaviors of the corroded specimens were studied, and the test results of Table 6 show decreases of (33%) and (29%) for the beam specimens (BMCF) and (BRCF) in comparison with the reference specimens. This implies that the decrease in the effective cross-sectional area of the bottom flange, due to corrosion, leads to loss of beam flexural strength, which in turn reduces the beam loading capacity.

Table 4. The ultimate load of tested Beams

Beam Coding	P_u (kN)	Pu/(Pu)r (%)
BMF*	90	-
BMCF	60	0.67
BMCSF	100	1.67
BRF*	70	0.78
BRCF	50	0.71
BRCSF	80	1.60

*Reference of monotonically and repeatedly tested beams.

4.3 Effect of Loading Type on (P_u)

When the load type changed from monotonic to repeated, the ultimate loads were reduced by (22%), (17%) and (20%) for the tested beam specimens (BRF), (BRCF) and (BRCSF), respectively in comparison with the corresponding monotonically tested beam specimens. The decline in strength is caused by the redistribution of loads during repeated processes, which causes energy dissipation and decreasing in ultimate load capacity.

4.4 Effect of Strengthening by CFRP

Two tested beam specimens (BMCSF) and (BRCSF) were strengthened by CFRP strips after being subjected to local damage by corrosion and then tested under monotonic and repeated loads respectively. The adopted strengthening technique, using CFRP strip, lead to an increase in the ultimate load by (67%) and (60%) for the tested beam specimens (BMCSF) and (BRCSF), respectively in comparison with un-strengthened corroded corresponding beam specimens (BMCF) and (BRCF). The presence of the CFRP in the longitudinal direction, at the bottom, creates an additional tension component that works with the tension force of the corroded bottom flanges to resist the bending stresses; as a result, the flexural strength and beam rigidity (stiffness) were increased significantly and as well as the ultimate loads in compared with the reference beam specimens (un-strengthened beams).

4.5 Load-Deflection Relationship

As mentioned before, the vertical displacements (deflections) were measured by using two dial gauges located underneath each tested beam specimen at the mid-span and quarter of span. The load-deflection curves of the tested beam specimens are plotted and provided in Fig. 7 to Fig.12. It can be observed from evaluating the relationship between the repeated load and deflection that the vertical deflection values increased as the number of repeated cycles increased, owing to a decrease in beam stiffness. The deflection values were increased in comparison with the reference specimens; the presence of corrosion leads to reduced beam flexural stiffness, and the results show an increase in vertical deflection. In the opposite direction, the strengthening by the CFRP strip leads to increased beam flexural stiffness and decreases the corresponding deflection as compared with the reference specimens.

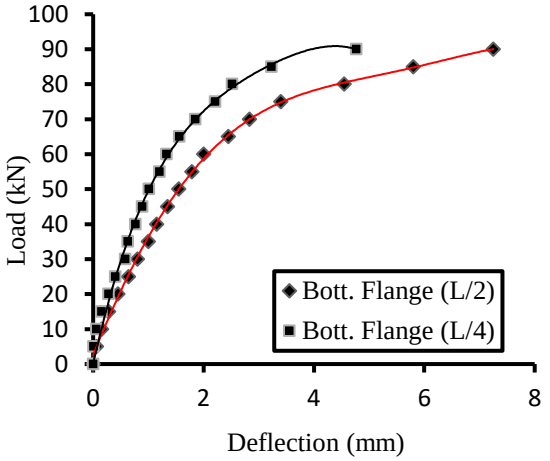

Figure 7. Load-deflection curve of the specimen (BMF)

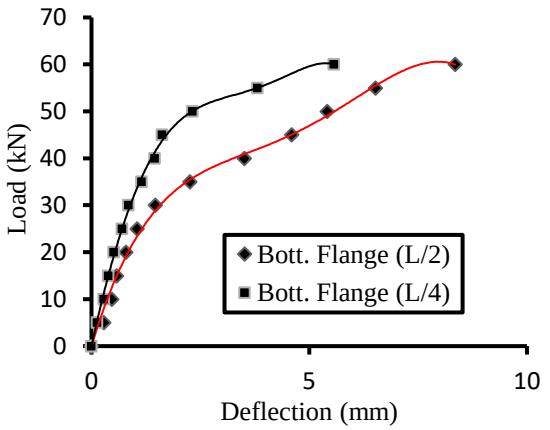

Figure 8. Load-deflection curve of the specimen (BMCF)

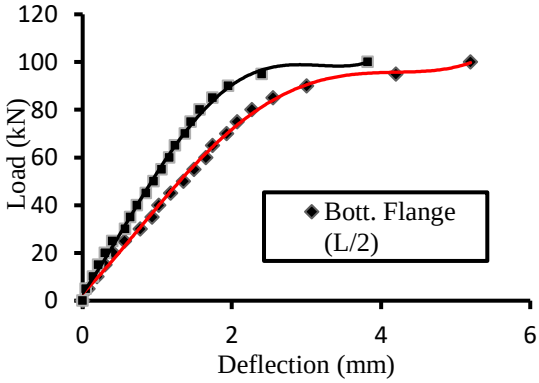

Figure 9. Load-deflection curve of the specimen (BMCSF)

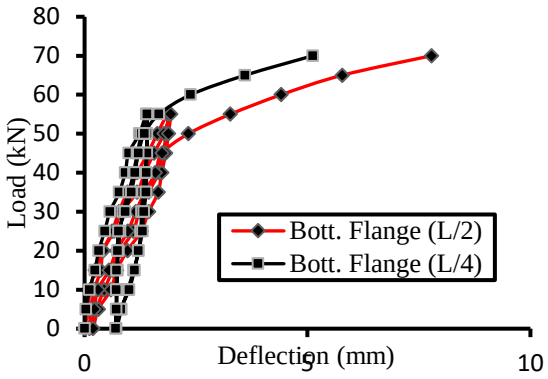

Figure 10. Load-deflection curve of the specimen (BRF)

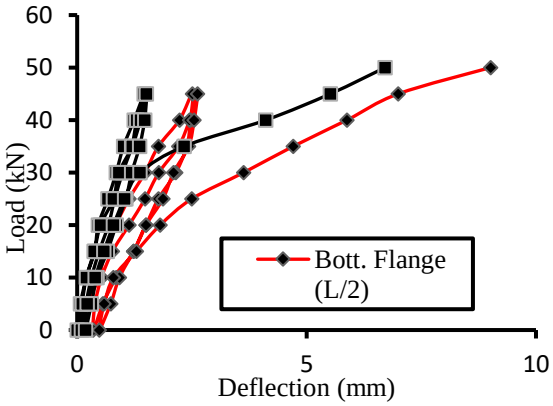

Figure 11. Load-deflection curve of the specimen (BRCF)

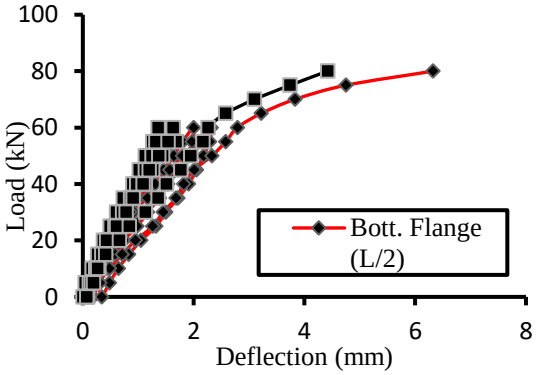

Figure 12. Load-deflection curve of the specimen (BRCSF)

4.6 Mode of Failure

The tested beam specimens (BMF), (BMCF), and (BRF) failed by a flexural mode of failure due to the yielding of the steel box section at the

bottom flange. Also, the tested beam specimen (BRCF) failed by flexural failure due to the yielding of the steel bottom flange and then by the local buckling failure of the top steel flanges. While for the corroded-strengthened beam specimens (BMCSF) and (BRCSF), the failures occurred due to rupture of the CFRP strips, which means that the CFRP strips reached their ultimate tensile strength before rupture.

Figure 13. Mode of failure of beam BMF

Figure 14. Mode of failure of beam BMCF

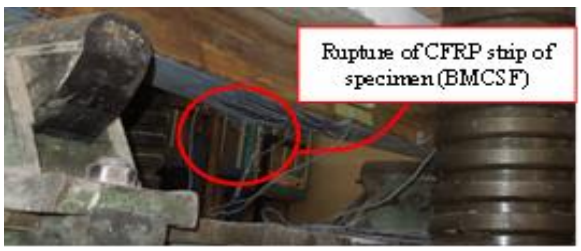

Figure 15. Mode of failure of beam BMCSF

Figure16. Mode of failure of beam BRF

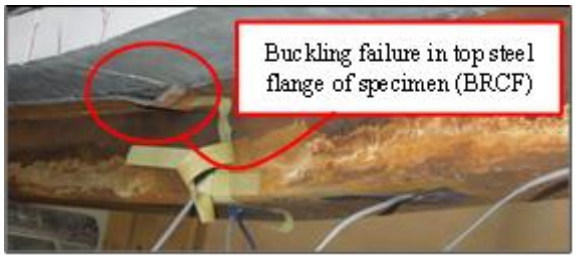

Figure 17. Mode of failure of beam BRCF

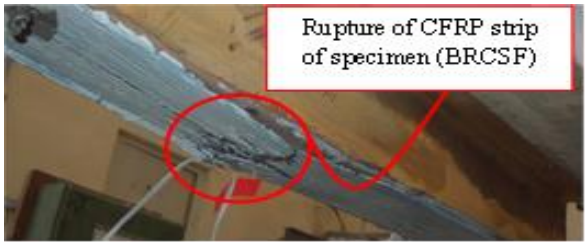

Figure 18. Mode of failure of beam BRCSF

5. Conclusions

The obtained results show that the ultimate loads were proportioned with the state of each tested beam specimen and the change of the applied loads from monotonic to repeated, lead to reduce the ultimate load by (17-22%). The decline in strength is produced by load redistribution during repeated loading, which causes energy dissipation as a result, the load capacity decreases, and the deflection increases. For the corroded beam specimens, the ultimate loads were decreased by (29-33%) in comparison with the corresponding reference specimens. This implies that the decrease in effective cross-sectional area of the bottom flange, due to corrosion, leads to loss of beam flexural strength, which in turn reduces the beam loading capacity. The ultimate loads for the strengthened beam specimens were increased by (60-67%) in comparison with the un-strengthened corroded corresponding beam specimens. The presence of the CFRP creates an additional tension component that works with the tension force of the corroded bottom flanges,

as a result, the flexural strength increased as well as the ultimate loads.

Conflict of interest

The authors affirm that there is no conflict of interest in the publishing of this work.

Author Contribution Statement

Author Ali Hameed Aziz: proposed the research problem and supervised the findings of this work. Author Ghufran Khudair Abbass: verified the analytical methods and investigated practically the effects of corrosion and performance of using CFRP strip at the bottom flange of a steel beam on the structural behavior of composite steel-concrete box beams. Results and contributions to the final manuscript were discussed by both authors.

6-References

1. Jack, C., and C. McCormac., (2012). *Structural Steel Design*. Library of Congress New Jersey., 5th ed. 2012, pp. 562.
2. Nashir, Muhammad. 2020. *Effect of Sulfuric Acid Concentration on The Corrosion Rate of ASTM A213-T12 Steel*. Pp. 213–217 in Key Engineering Materials. Vol. 867. Trans Tech Publ. https://doi.og/10.4028/kem.867.213.
3. Paneru, Nav Raj. 2018. "Prestressed Carbon Fiber Reinforced Polymer (CFRP) Tendons in Bridges."M.SC. Thesis, University of Toledo. https://doi.org/10.14359/5653
4. Sayed-Ahmed, Ezzeldin Yazeed. 2001. *Behaviour of Steel and (or) Composite Girders with Corrugated Steel Webs*. Canadian Journal of Civil Engineering 28(4):656–72. https://doi.org/10.1139/l01-027.
5. Al-Saidy, Abdullah H., F. W. Klaiber, and T. J. Wipf. 2004. *Repair of Steel Composite Beams with Carbon Fiber-Reinforced Polymer Plates.* Journal of Composites for Construction 8(2), pp. 656-672. https://doi.org/10.1061/(asce)1090-0268(2004)8: 2(163)
6. Liang, Qing Quan, Brian Uy, Mark A. Bradford, and Hamid R. Ronagh. 2005. *"Strength Analysis of Steel-Concrete Composite Beams in Combined Bending and Shear."* Journal of Structural Engineering 131(10), pp.1593–1600. https://doi.org/10.1061/(asce)0733-9445(2005)131:10(1593)
7. Ibrahim, Amer M., and Qussay W. Ahmed. 2013. "*Nonlinear Analysis of Simply Supported Composite Steel-Concrete Beam.*" Diyala Journal of Engineering Sciences 6(3), pp.107–126. https://doi.org/10.24237/djes.2013.06308
8. W. M. A. W. Azmi, "*Study on Effects of Soil Properties Towards Corrosion of Carbon Steel Pipeline."* University Malaysia Pahang, 2014. https://doi.org/10.1109/afrcon.2015.7331942
9. Y. Bao, M. Gulasey, C. Guillaume, N. Levitova, A. Moraes, and C. Satter, "*Structural capacity analysis of corroded steel girder bridges,"* 2018. https://doi.org/10.11159/iccste18.118
10. Ibrahim, Amer M., Wissam D. Salman, and Fahad M. Bahlol. 2019. *"Flexural Behavior of Concrete Composite Beams*

with New Steel Tube Section and Different Shear Connectors." Tikrit Journal of Engineering Sciences 26(1), pp.51–61. https://doi.org/10.24237/djes.2019.12404

11. Iraqi Specifications No. (5), "*Portland Cement*", the Iraqi Central Organization for Standardization and Quality Control, Baghdad-Iraq, 1984.
12. Iraqi Specifications No. (45), "*Aggregates from Natural Sources for Concrete and Building Construction*", the Iraqi Central Organization for Standardization and Quality Control, Baghdad-Iraq, (1984).
13. ASTM Designation C494–99a, "*Standard Specification for Chemical Admixtures for Concrete*", American Society for Testing and Material, Philadelphia, Pennsylvania, USA.
14. ASTM-A 370–02, "*Standard Test Methods and Definitions for Mechanical Testing of Steel Products*", American Society for Testing and Material, Philadelphia, Pennsylvania, USA.
15. ASTM A615/A615M, "*Standard Specification for Deformed and Plain Carbon-Steel Bars for Concrete Reinforcement*", American Society for Testing and Material, Philadelphia, Pennsylvania, USA.
16. ASTM C138- 17, "*Standard Test Method for Density (Unit Weight), Yield, and Air Content (Gravimetric) of Concrete*", American Society for Testing and Material, Philadelphia, USA.
17. BS 1881-116, Method for determination of compressive strength of concrete cubes, British Standards Institute, London, 1983.
18. ASTM C39-01, (2001), "*Standard Test Method for Compressive Strength of Cylindrical Concrete Specimens*", American Society for Testing and Material, Philadelphia, USA.
19. ASTM C496 – 96, (1996), "*Standard Test Method for Splitting Tensile Strength of Cylindrical Concrete Specimens*", American Society for Testing and Material, Philadelphia, USA.
20. ASTM C78-02, "*Standard Test Method for Flexural Strength of Concrete (Using Simple Beam with Third-Point Loading*", American Society for Testing and Materials, Philadelphia, USA.